RESEARCH ARTICLE

Macromolecular Bioscience
www.mbs-journal.de

Inhibition of the Fibrillation of Amyloid A$\beta_{1\text{-}40}$ by Hybrid-Lipid-Polymer Vesicles

*Newton Sen, Caroline Haupt, Gerd Hause, Kirsten Bacia, and Wolfgang H. Binder**

The transformation of functional proteins into amyloidic plaques is responsible for the impairment of neurological functions in patients fallen victim to debilitating neurological conditions like Alzheimer's, Parkinson's, and Huntington's diseases. The nucleating role of amyloid beta (A$\beta_{1\text{-}40}$) peptide into amyloids is well established. Herein, lipid hybrid-vesicles are generated with glycerol/cholesterol-bearing polymers aiming to alter the nucleation process and modulate the early phases of A$\beta_{1\text{-}40}$ fibrillation. Hybrid-vesicles (±100 nm) are prepared by incorporating variable amounts of cholesterol-/glycerol-conjugated poly(di(ethylene glycol)$_m$acrylates)$_n$ polymers into 1,2-dioleoyl-sn-glycero-3-phosphocholine (DOPC) membranes. The in vitro fibrillation kinetics coupled to transmission electron microscopy (TEM) is employed to investigate the role of hybrid-vesicles on A$\beta_{1\text{-}40}$ fibrillation without destroying the vesicular membrane. Both polymers, when embedded in hybrid-vesicles (up to 20%) significantly prolonged the fibrillation lag phase (t_{lag}) compared to a small acceleration in the presence of DOPC vesicles, irrespective of the amount of polymers inside the hybrid-vesicles. Along with this notable retardation effect, a morphological transformation of the amyloid's secondary structures to amorphous aggregates or the absence of fibrillar structures when interacting with the hybrid-vesicles is confirmed by TEM and circular dichroism (CD) spectroscopy.

1. Introduction

Fibrillar aggregation of proteins has received increasing attention due to the involvement of such proteins in a variety of neurodegenerative diseases, such as Alzheimer's, Parkinson's, and Prion diseases. The assembly of the amyloid peptides A$\beta_{1\text{-}40/42}$ in particular has been studied in more detail, especially in view of forming oligomeric forms of these polymorphic aggregates, which are considered toxic to neurons.[1] During pathological aggregation, the monomeric and soluble peptides or proteins are converted into oligomers and finally into amyloid fibrils[3,4] similar to the in vitro formation of protein fibrils.[2] Mechanistically, the in vitro aggregation process is characterized by a nucleation-dependent sigmoidal growth phase, where the region preceding the typically observed steep increase in fluorescence intensity in ThT-assays is termed as the lag phase, during which (short-lived) oligomers composed of only a few monomers are formed, from wherein surface induced polymerization monomers continues from previously formed aggregates.[2,3] A plethora of different small molecules,[4–9] polymers,[10–20] peptides[17,21] and proteins,[22,23] nanoparticles, and nanomaterials[24,25] have been shown to influence the aggregation resulting in modified growth-curves of Aβ fibril formation in vitro, presumably interacting both, specifically (via eg. intermolecular hydrogen bonds) and nonspecifically with the fibrillation process.[26,27] Especially amphiphilic molecules such as lipids or surfactants and their aggregates (micelles[9] and membranes[28,29] or vesicles[30]) are strongly modulating the assembly of Aβ. Thus surfactants (such as sodium dodecyl sulfate, SDS), proposed to change the pathway of assembly at concentrations below the critical micelle concentration (CMC), lead to a change in the conformational state of the monomeric species (recorded as an increase in α-helix content as measured by circular dichroism (CD) spectroscopy[31]) by complex formation between A$\beta_{1\text{-}40}$ and the surfactant[32] or in Aβ_{42}.[33] Negatively charged membranes have been demonstrated to exert a strong influence on amyloid aggregation, proposed to accelerate the fibrillation by electrostatic interaction, whereas zwitterionic lipids exert a strong effect on the oligomerization,[9] but only a minor influence on Aβ aggregation.[30,34] Due to the fundamental medical importance of lipids in view of fibrillation of A$\beta_{1\text{-}40}$[35–37] the composition of vesicular membranes

N. Sen, W. H. Binder
Macromolecular Chemistry
Institute of Chemistry
Faculty of Natural Science II (Chemistry, Physics and Mathematics) Martin Luther University Halle-Wittenberg
von-Danckelmann-Platz 4, D-06120 Halle, Germany
E-mail: wolfgang.binder@chemie.uni-halle.de

C. Haupt, K. Bacia
Biophysical Chemistry
Institute of Chemistry and Charles-Tanford Protein Center
Martin Luther University of Halle-Wittenberg
06120 Halle (Saale), Germany

G. Hause
Biocenter
Martin-Luther University Halle-Wittenberg
Weinbergweg 22, D-06120 Halle (Saale), Germany

The ORCID identification number(s) for the author(s) of this article can be found under https://doi.org/10.1002/mabi.202200522

DOI: 10.1002/mabi.202200522

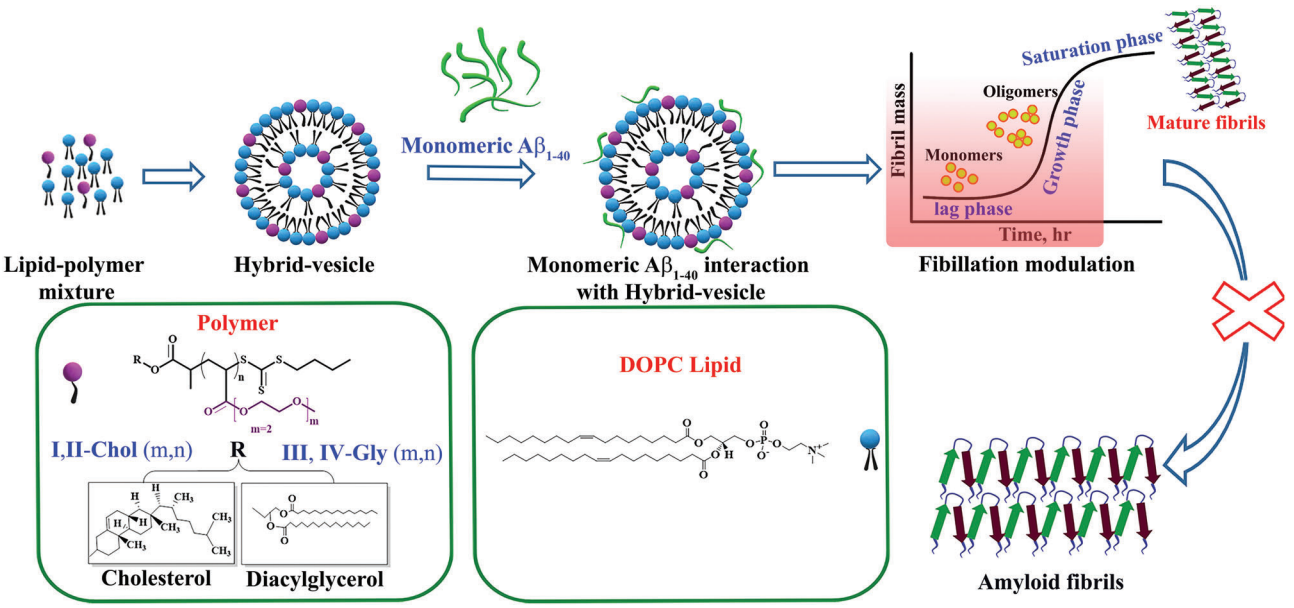

Figure 1. Concept showing the inhibition of amyloid A$\beta_{1\text{-}40}$ fibrillation by modified vesicles containing embedded cholesterol/diacylglycerol-modified-poly(di(ethylene glycol)$_m$acrylates)$_n$. Mixtures of the polymers **I**, **II**, **III** and **IV** (5–20 mol%) were generated with the lipid (DOPC), subsequently forming hybrid-vesicles via film-rehydration and extrusion. The inhibition of A$\beta_{1\text{-}40}$ fibrillation was then investigated in view of the polymers, the lipid as well as the used concentration of the polymers inside the vesicles.

has shown to exert a considerable influence on aggregation, in particular the presence of cholesterol[37–42] and other lipid membrane components, also in view of size[43] and their role in surface-guided nucleation processes.[43–46]

We have recently demonstrated that certain amphiphilic polymers are able to inhibit fibrillation of A$\beta_{1\text{-}40}$.[47–50] To this end a series of different polymers, displaying a variable hydrophilicity-hydrophobicity profile, induces a significant reduction of A$\beta_{1\text{-}40}$ fibrillation based on their end groups or side chains.[47] Thus especially polymers bearing hydrophobic anchors, such as novel lipid-polymer conjugates, were shown to display a strong inhibitory effect, partially also linked to conformational transitions induced by temperature. The conjugates containing hydrophobic lipid anchors (for example cholesterol, diacylglycerol) inhibited A$\beta_{1\text{-}40}$ fibrillation significantly (both lag, t_{lag} and half times, $t_{1/2}$) as indicated by in vitro kinetic studies and transmission electron microscopy (TEM).[50]

This motivated to investigate the fibrillation behavior of some of these lipid-polymer conjugates directly embedded into artificial vesicles, designed as a hybrid-vesicles containing the cholesterol/diacylglycerol-modified-poly(di(ethylene glycol)$_m$acrylates)$_n$, in more detail (see **Figure 1**). The polymers, which bear hydrophilic oligo (ethylene) acrylate chains comparable to previously reported polymers, are intended to carry membrane-anchoring groups at their chain end (cholesterol, diacylglycerol) to reach a stable embedding into the lipid bilayer membrane. Thus in our current approach, the polymers, now embedded in DOPC vesicles in amounts up to 20 mol%, result in a dense layer on the outside of the vesicles. Conceptually, we incorporated these polymers into 1,2-dioleoyl-sn-glycero-3-phosphocholine (DOPC) vesicles to probe their influence on the fibrillation of native A$\beta_{1\text{-}40}$. We put a detailed effort into the preparation of these hybrid-vesicles with varying polymer amounts, as well as into the final effects observed during fibrillation. Finally, amyloid fibrils were investigated by electron microscopy (TEM) and circular dichroism (CD)-spectroscopy.

2. Result and Discussion

2.1. Synthesis of the Polymers

Polymers (**I–IV**) bearing the cholesterol/diacylglycerol-modified-poly(di(ethylene glycol)$_m$acrylates)$_n$ were prepared by RAFT-polymerization as described previously, using appropriate RAFT-agents bearing the cholesteryl (**I**, **II**)/diacylglycerol units (**III**, **IV**).[50] Details of the synthesis reported in the Supporting Information (SI), selected details on the achieved molecular weights (M_n), polydispersities (M_w/M_n) as well as a thorough characterization by NMR-spectroscopy and MALDI-TOF have been reported earlier and are presented in **Table 1**. Thus, it is possible to reach an excellent end group fidelity, with the two main end groups, cholesteryl- and diacylglycerol completely present in all polymer chains, as exemplified by MALDI-TOF and NMR. We here have focused on only a single set of polymers to investigate their subsequent incorporation into DOPC vesicles, where hydrophilicity was restricted to only two ethylene oxide (EO)-units in the sidechain of the acrylate polymers. We were able to reach molecular weights ranging from 2200 to 9000 Da, as well as successfully implement the respective cholesteryl- and diacylglycerol units at the chain end of all polymers. Most polymers display lower critical solution transitions, as indicated in Table 1.

2.2. Formation of the Hybrid-Vesicles

We subsequently turned our attention to the formation of hybrid-vesicles, composed of the polymers in mixture with DOPC as

Table 1. Properties of the used thermoresponsive polymers **I, II, III, and IV** to understand their influence on A$\beta_{1\text{-}40}$ fibrillation after embedding into hybrid liposomes composed of DOPC. Polymers are further specified with respect to their degree of polymerization (n) and the length of their ethylene oxide (EO) sidechain (m).[50]

Entry	Polymer Name	End group	n[a)]	m[b)]	$M^{a}_{n,\,NMR}$ (gmol^{-1})	T_{cp}[c)] (°C)
1	**I-Chol** (m, n)	Cholesterol	9	2	2200	Above 90
2	**II-Chol** (m, n)		48	2	9000	42. 8
3	**III-Gly** (m, n)	Glycerol	10	2	2550	Above 90
4	**IV-Gly** (m, n)		44	2	8450	39. 4

[a)] Degree of polymerization (n) and molecular weight (M_n) determined from ^{1}H-NMR in $CDCl_3$; [b)] No. of ethylene oxide (EO) (m) units maintained from the diethylene glycol mono ethyl ether (DGME) monomer; [c)] Polymer cloud point temperatures (T_{cp}) determined in a 150 mM NaCl-solution supplemented 50 mM Na_2HPO_4 buffer at pH 7. 4.

Table 2. Mixing ratios of the lipid and the different concentrations (provided in mol%) of (**I**, **II**, **III,** and **IV**) polymers inside the hybrid vesicles.

Entry	Polymer name	End group	Lipid and conc. of lipid (mM)	Polymer conc.[a)] (mol %)	Molar ratio [Lipid]/ [Polymer]
1	**I-Chol** (9, 2)	Cholesterol	DOPC (1. 5 mM)	5	20
2				10	10
3				15	6.7
4				20	5
5	**II-Chol** (48, 2)			5	20
6				10	10
7				15	6.7
8				20	5
9	**III-Gly** (10, 2)	Glycerol		5	20
10				10	10
11				15	6.7
12				20	5
13	**IV-Gly** (44, 2)			5	20
14				10	10
15				15	6.7
16				20	5

[a)] Polymer mixed with DOPC in a chloroform: methanol (2:1) mixture.

the lipid component. Based on previously reported standard methods (formation of a mixed lipid film, rehydration, extrusion through 100 nm polycarbonate membranes)[51,52] we were able to generate a number of different hybrid vesicles, as shown in **Table 2** and the Supplementary Table S1. Thus, ratios of the embedded polymers ranging from ≈5 mol% to 20 mol% inside the vesicles were achieved.

The method yielded stable mixed vesicles as shown in **Figure 2**A-F. Cryo-TEM (cryo-transmission electron microscopy) images displayed vesicles in the desired size range, supported by dynamic light scattering (DLS) measurements showing narrow size distribution curves with maxima of ≈100 nm. The images of Figure 2A-F and Figure S7, see Supporting Information, show the hybrid vesicles embedded with variable molar percentages of **I-Chol** (9, 2), **II-Chol** (48, 2), **III-Gly** (10, 2) and **IV-Gly** (44, 2) polymers with a size distribution profile in Figure S8, see Supporting

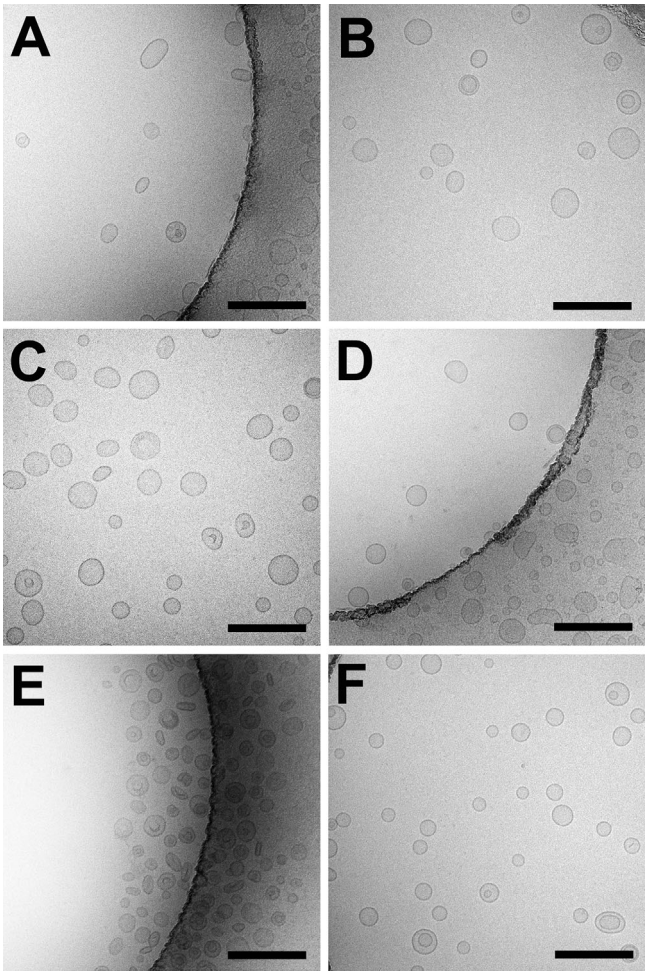

Figure 2. Cyro-EM images of hybrid vesicles containing A) **I-Chol** (9, 2) polymer (5%), B) **II-Chol** (48, 2) polymer (5%), C) **II-Chol** (48, 2) polymer (20%), D) **III-Gly** (10, 2) polymer (10%) E) **IV-Gly** (44, 2) polymer (5%) and F) **IV-Gly** (44, 2) polymer (20%) with a scale bar of 250 nm.

Information. These hybrid-vesicles were stable for up to several hours at 4 °C, a sufficiently long time for investigating the subsequent assays to study amyloid fibrillation.

An important issue in this endeavor was to justify the precise amount of the polymers truly incorporated into the hybrid-vesicles. To this end, several experiments were conducted to prove that the polymers have been incorporated into the vesicular membrane and are not just present as a physical mixture.

We used ^{31}P-NMR spectroscopy of the lipids to check for changes during the incorporation of the polymers into the hybrid-vesicles. ^{31}P-NMR spectroscopy is known to be highly sensitive to the environment of the lipid head group,[53–55] especially in view of the lipid head groups and the surrounding polarities. Figure S1B (see Supporting Information) shows results for the ^{31}P-NMR of intact DOPC vesicles containing different amounts of incorporated polymers. Thus the formation of hybrid-vesicles is clearly proven by changes in the chemical shift from −0.79 ppm for native DOPC vesicles to higher chemical shift-values when the polymer is incorporated inside the vesicles. Incorporation of the polymers in amounts ranging from 5% up to 15% showed changes in

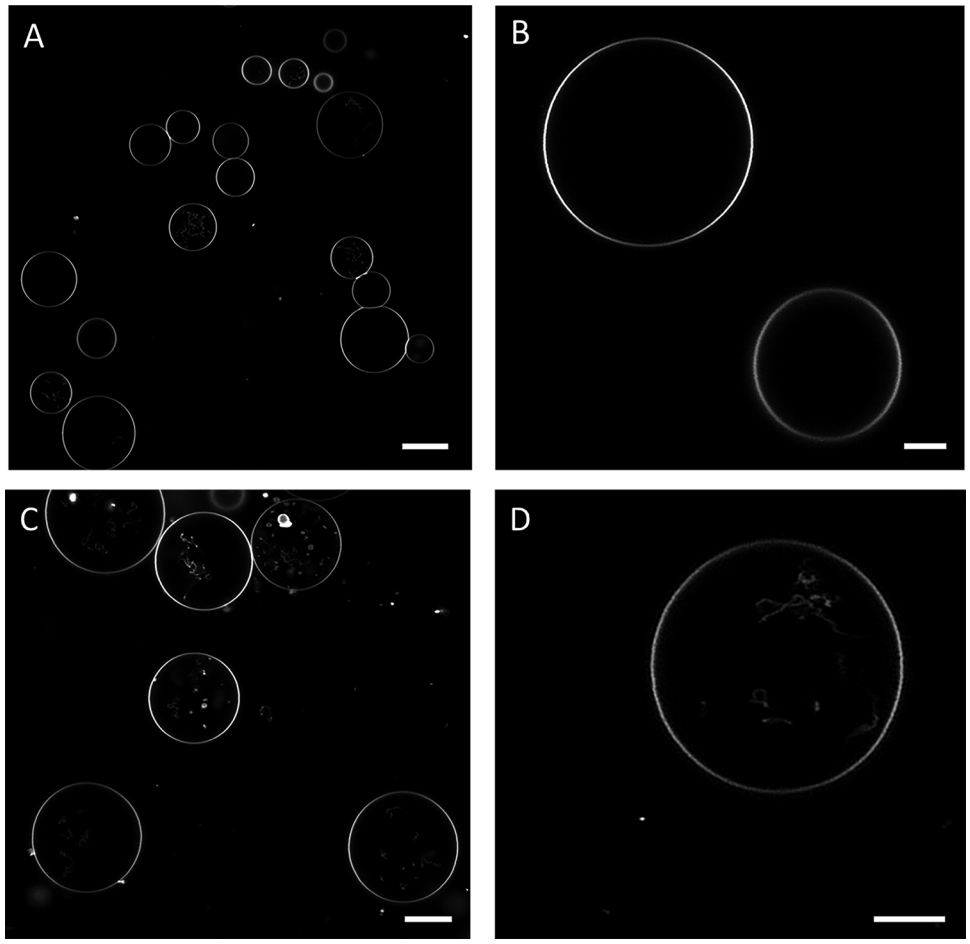

Figure 3. Confocal microscopy slice images of pure DOPC GUVs and hybrid-GUVs at room temperature using the lipophilic fluorescent tracer $DiIC_{18}$ to visualize the lipid bilayer and potential membrane heterogeneities. Panel A) represents pure DOPC GUVs; B) shows the confocal image of a single DOPC GUV. The gradual change in fluorescence along the perimeter is due to the polarization of the laser and the orientation of the dye in the lipid bilayer.[58] The fluorescence follows the expected pattern. C,D) depict the hybrid-GUVs composed of DOPC and **II-Chol** (48, 2) polymer, with 5 mol% of **II-Chol** (48, 2) polymer during the initial mixing of DOPC and **II-Chol** (48, 2). The images show the same homogeneous distribution of the fluorescent dye as in GUVs prepared from DOPC only, with no defects or signs of phase separation. Scale bars: (**A**) 20 µm, (**B**) 5 µm, (**C**) 10 µm, (**D**) 5 µm.

the ^{31}P-NMR resonances, indicative of the successful incorporation of the polymers inside the vesicle-membrane. Those changes can be attributed to the different polar environments exerted by the hydrophilic parts of the polymers, now incorporated into the vesicular entities.

We also investigated changes in the zeta-potential (ζ) after incorporating various amounts (5 mol% to 20 mol%) of **I-Chol** (9, 2), **II-Chol** (48, 2), **III-Gly** (10, 2) and **IV-Gly** (44, 2) polymer into the DOPC vesicles (see Figure S2, Supporting Information). In the case of **I-Chol** (9, 2), and **II-Chol** (48, 2) polymer-bearing hybrid-DOPC vesicles, there are smaller changes in the ζ-potential with increasing amounts of the polymers. A final proof was gained by quantifying the amounts of polymers inside the vesicles by separation of freshly formed vesicles from solution by centrifugation, subsequent removal of the buffer, and quantification by ^{1}H-NMR spectroscopy. The values of the initial mixtures fall close to the values obtained after vesicle isolation (see Figure S1A, Supporting Information), proving the true incorporation of the polymers into the vesicular bilayer membranes.

We also visualized the membranes of hybrid vesicles by confocal fluorescence microscopy of fluorescently labeled giant unilamellar vesicles (GUVs) to check for an eventual membrane phase separation or unusual membrane morphologies which could potentially be caused by the polymer.[56,57] In the confocal images of hybrid-GUVs (5 mol% of **II-Chol** (48, 2) polymer), labeled with the lipophilic 1,1"-dioctadecyl-3,3,3",3'-tetramethylindocarbocyanine perchlorate ($DiIC_{18}$) dye (see **Figure 3**) no membrane inhomogeneities could be seen.

2.3. Inhibition of A$\beta_{1\text{-}40}$ Fibrillation by Added Hybrid-Vesicles

To examine the impact of tunable hybrid-vesicles on amyloid fibrillation, thioflavin T (ThT) based in vitro fibrillation kinetics assays were used to investigate quantitatively the hybrid-vesicles´ influence on A$\beta_{1\text{-}40}$ peptide fibrillation. To perform the kinetic investigations, the monomeric peptide (10 µM) was mixed physically with the hybrid-vesicles in a 150 mM NaCl containing

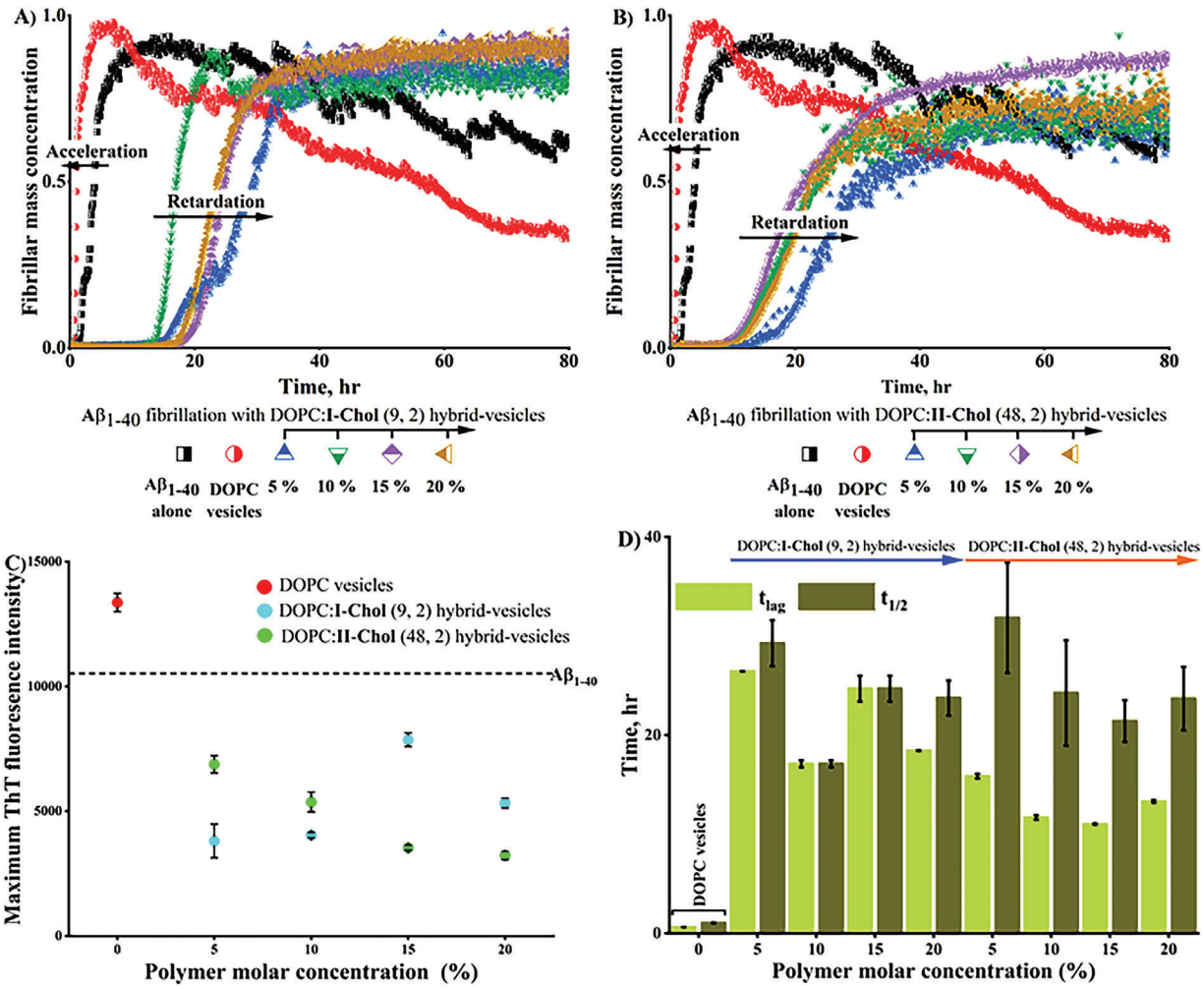

Figure 4. Influence of hybrid-vesicles composed of DOPC and variable percentages (up to 20 mol%) of cholesterol end group bearing A) **I-Chol** (9, 2) and B) **II-Chol** (48, 2) polymers on $A\beta_{1\text{-}40}$ fibrillation. 75 μM (5 mol%), 150 μM (10 mol%), 225 μM (15 mol%), and 300 μM (20 mol%) polymers were embedded during hybridization of 1.5 mM DOPC lipid. Fibrillation of $A\beta_{1\text{-}40}$ is monitored via the ThT fluorescence intensity in a 50 mM Na_2HPO_4 buffer containing 150 mM NaCl at pH 7.4 and 37 °C with repeated agitation. The fibrillation profile of $A\beta_{1\text{-}40}$ (10 μM) in the presence of hybrid-vesicles (≈100 nm) is monitored by ThT fluorescence intensity with time. A summary of the lag time, t_{lag} and the half time, $t_{1/2}$, are obtained from the fibrillation kinetic assays and plotted against the embedded polymer concentrations in hybrid-vesicles, further compared to pure DOPC vesicles D). Maximal fibril mass formation, derived from the main ThT fluorescence intensity of Figure S3, Supporting Information, both liposomes and hybrid liposomes are compared with native $A\beta_{1\text{-}40}$ (dotted black line) with indicated error bars C). The error bars of all figures indicate the standard deviation among the independent replicates.

50 mM Na_2HPO_4 buffer at pH 7.4 and 37 °C. ThT fluorescence intensity increased with the propagation of amyloid $A\beta_{1\text{-}40}$ fibrillation and therefore the ThT fluorescence intensity at $\lambda = 488$ nm was used to track the aggregation kinetics as well as to decipher the influence of lipid vesicles hybridization on amyloid fibrillation. Both cholesterol (**I**, **II**) and glycerol (**III**, **IV**), polymers were used for the hybridization of DOPC vesicles to study their influence on $A\beta_{1\text{-}40}$ fibrillation.

2.3.1. Retardation of Fibrillation by Cholesterol-Modified-Poly(Di(Ethylene Glycol)$_m$Acrylates)$_n$ Embedded in Hybrid-Vesicles

To investigate the effect of hybrid-vesicles on peptide fibrillation, firstly the fibrillation kinetics of the $A\beta_{1\text{-}40}$ peptide was monitored in the presence of native, polymer-free DOPC vesicles. By comparing the kinetics in the presence or absence of DOPC vesicles, a slight acceleration of fibrillation was observed with pure DOPC vesicles, as revealed by the faster lag time (t_{lag}) changing from ≈2 h to 1 h.[50] (**Figure 4**A,B).

Subsequently, the cholesterol-bearing polymers **I-Chol** (9, 2) and **II-Chol** (48, 2), with molecular weights of 2200 and 9000 Da, were embedded into the hybrid-DOPC vesicles. Variable molar percentages up to 20% were probed to investigate whether the end group of the polymer, the molecular weight, and the percentage of the incorporated polymers exert an influence on fibrillation. From the fibrillation assays (see Figure 4), a significant inhibition effect from the polymers (both **I**, **II**) bearing hybrid-vesicles was clearly observed, proving that both molecular weights of the polymers in the hybrid vesicles inhibited the fibril formation.

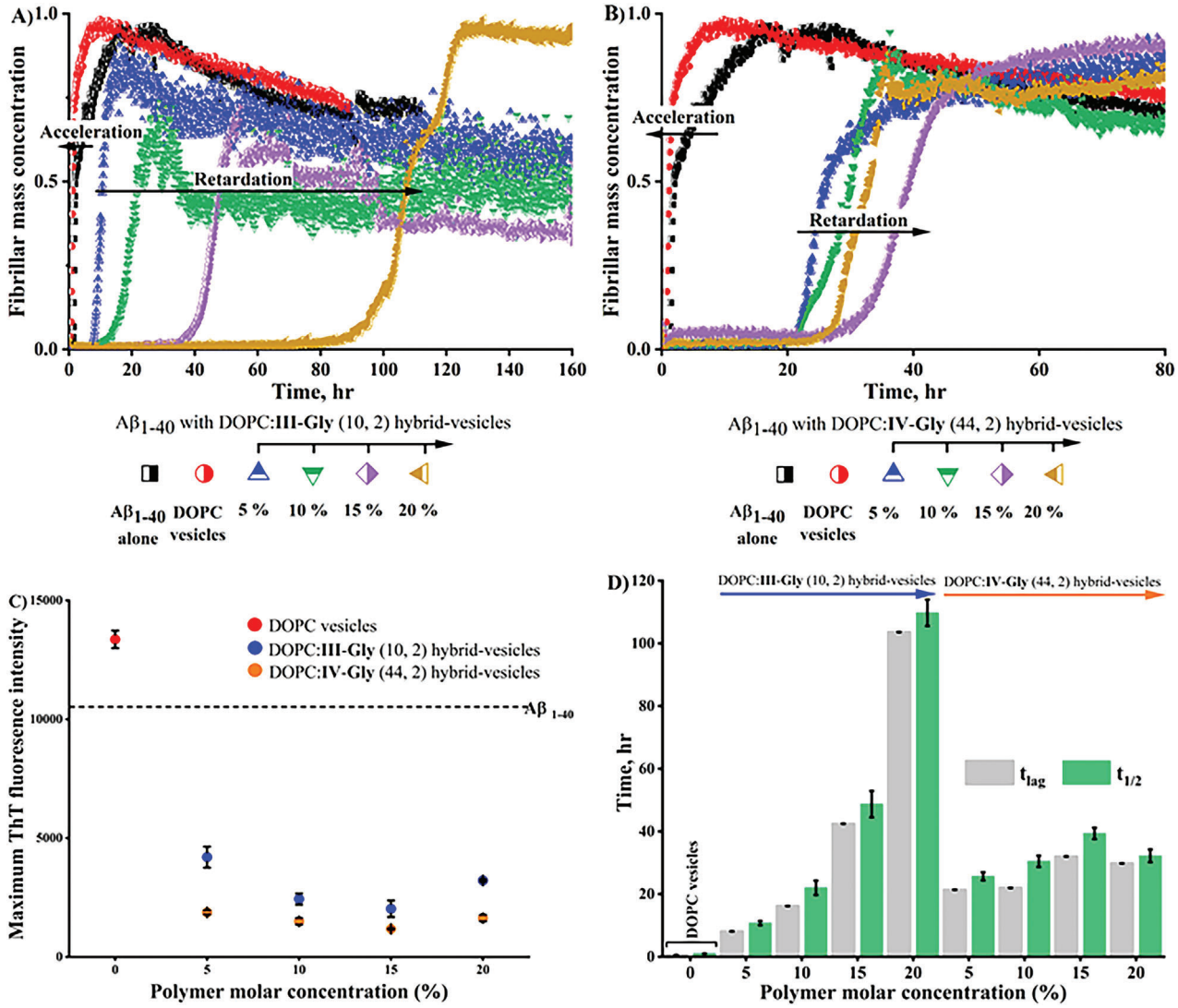

Figure 5. Impact of embedded A) **III-Gly** (10, 2) and B) **IV-Gly** (44, 2) polymers in DOPC-hybrid vesicles on $A\beta_{1\text{-}40}$ (10 µM) fibrillation. The ThT kinetics were performed in 150 mM NaCl supplemented Na_2HPO_4 buffer (pH 7.4) at 37 °C in shaking mode. Influence of the polymers (5 mol% to 20 mol%) incorporated hybrid liposomes (≈100 nm) on $A\beta_{1\text{-}40}$ fibrillation are plotted against the time and compared to pure DOPC (1.5 mM) vesicles. Fibril load (calculated from Figure S3, Supporting Information) after incubation with hybrid- and pure DOPC-vesicles are presented against the respective molar concentrations and compared to native $A\beta_{1\text{-}40}$ (dotted black line) C). t_{lag} and $t_{1/2}$, derived from fibrillation kinetics, of hybrid-vesicles are compared to DOPC vesicles D). The errors of the replicated measurements indicate with bars. Polymer concentration mentioned in Figure 4 was incorporated for the hybridization of 1.5 mM DOPC.

With an increasing molecular weight of the polymers, the fibrillation time (t_{lag} and $t_{1/2}$) was significantly increased. A steeper slope of the kinetic assays was clearly observed with the hybrid-vesicles bearing **I-Chol** (9, 2) polymer compared to the **II-Chol** (48, 2) polymer embedded hybrid-vesicles. Probably the **II-Chol** (48, 2)-vesicles modulate the early nucleation processes of fibrillation, which led to changes in fibrillation behavior along with pronounced inhibition impact. All embedded polymer concentrations (5 mol% to 20 mol%) within the hybrid-DOPC vesicles retarded the fibrillation notably compared to native $A\beta_{1\text{-}40}$ alone.

The strongest inhibition was asserted by the 5 mol% polymer containing hybrid-vesicles for both polymers. An increased lag time of ≈27 h and ≈16 h, as well as an elongated half time of ≈30 h and ≈32 h, was observed respectively for **I-Chol** (9, 2) and **II-Chol** (48, 2) polymers in hybrid-vesicles, compared to $A\beta_{1\text{-}40}$ (t_{lag} ~ 2 h and $t_{1/2}$ ~ 4 h) without any hybrid-vesicles. A substantial delay of fibrillation time was observed even with higher amounts (10, 15, and 20 mol%) of polymers in DOPC-hybrid vesicles. The elongated fibrillation for the above-mentioned polymers bearing hybrids was quantified with a delayed lag time of 2 h to 10 h for the **I-Chol** (9, 2) polymer and 3 hr to 5 hr for the **II-Chol** (48, 2) polymer (Figure 4A,B). Another important aspect of fibrillation is the amount of fibrils that can be extracted from the raw ThT intensities when the intensities reach a maximum (see Supplementary Figure S3, Supporting Information). The total amount of fibrils is increased significantly for native DOPC

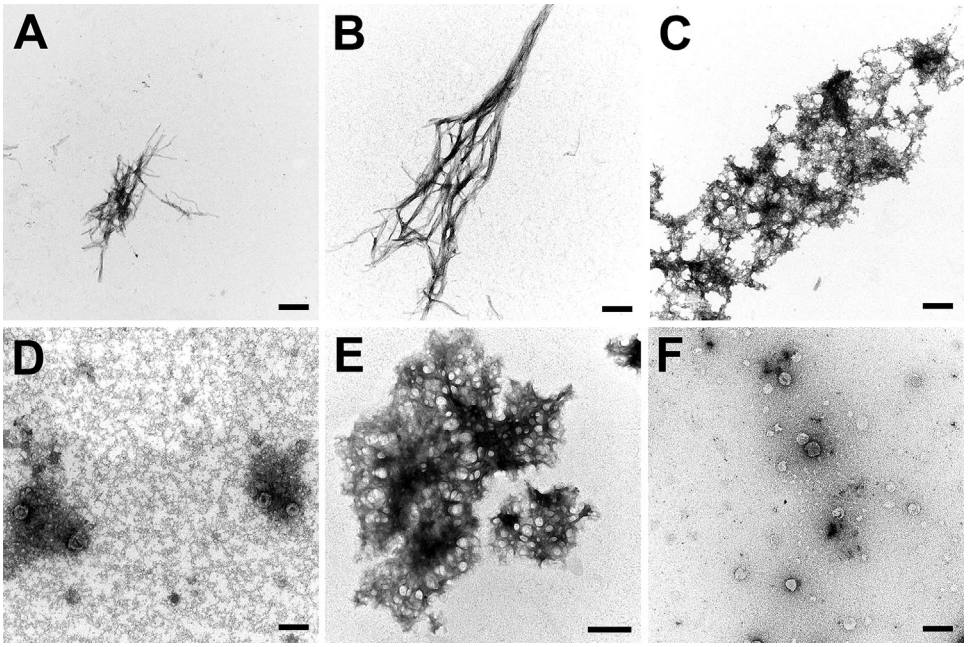

Figure 6. TEM images were recorded after $A\beta_{1\text{-}40}$ fibrillation in ThT assays using a negative stain of uranyl acetate. The representative images of $A\beta_{1\text{-}40}$ fibrillation either in the absence of liposomes A) or in the presence of DOPC liposomes B), and hybrid liposomes containing 10% of **I-Chol** (9, 2) C), 20% of **II-Chol** (48, 2) D), 5% of **III-Gly** (10, 2) E), 10% of **IV-Gly** (44, 2) F) polymers. The scale bar in **E** represents 500 nm; all other bars represent 250 nm.

vesicles compared to the native $A\beta_{1\text{-}40}$, whereas the amount of mature fibrils dropped substantially for all hybrid materials irrespective of the amounts and nature of polymers embedded (Figure 4C). Depending on the presentation of the polymer outside of the vesicles we believe that an efficient interaction of the polymer-chain with the nucleating amyloid proteins is guided by both, hydrophobic interaction towards the amyloid $A\beta_{1\text{-}40}$ proteins and a steric stabilization effect (stealth-effect), the latter being concentration dependent. Similar to steric stabilization a concentration of ≈5 mol% is the most efficient concentration to exert steric stabilization towards the nucleating amyloid $A\beta_{1\text{-}40}$ proteins by the then extended polymer chains.

2.3.2. Fibrillation Inhibition by Diacylglycerol-Anchored-Poly(Di(Ethylene Glycol)$_m$Acrylates)$_n$ Polymers in Hybrids

The retardation of fibrillation was similarly observed for the other investigated hybrid-vesicles (bearing the **III**-Gly (10, 2) and **IV**-Gly (44, 2) polymers). The inhibition of fibrillation was pronounced for all the investigated concentrations (up to 20 mol%) of these glycerol end group-bearing polymers in DOPC vesicles (see **Figure 5**), with the most significant inhibitory effect at the highest concentration, especially with the polymer **III-Gly** (10,2).

Among the investigated polymer concentrations in vesicles (5 mol% to 20 mol%), the strongest retardation of fibrillation was observed for those containing 15 mol% and 20 mol% of both **III-Gly** (10, 2) (M_n = 2550 g mol^{-1}) and **IV-Gly** (44, 2) (M_n = 8450 g mol^{-1}) polymers, by a factor of ≈27 for 15 mol% **III-Gly** (10, 2), ˜66 for 20 mol% **III-Gly** (10, 2), ≈20.4 for 15 mol% **IV-Gly** (44, 2) and ≈20 for 20 mol% **IV-Gly** (44, 2) bearing vesicles, respectively (see Figure 5D). Considering the amount of fibrils in aggregates, a significant reduction of fibrils was quantified from the unnormalized fibrillation kinetics (Figure 5C andFigure S3, Supporting Information). The reduction of fibrils became more predominant in the case of glycerol-anchored polymers in hybrid-vesicles, when compared to the cholesterol-anchored polymer containing vesicles (see Figure 4C and Figure 5C). Again the most hydrophobic polymer (**III-Gly** (10,2)) showed the strongest inhibitory effect, assuming that there might be an influence from the very high cloud temperature (T_{cp} > 90 °C) of the polymer, forming an external conformation of the polyethylene oxide (PEO)-part.

As the fibrillation kinetic assays clearly prove the inhibitory effect of hybrid-vesicles, we further investigated morphological changes of $A\beta_{1\text{-}40}$ aggregates induced by the hybrid-vesicles. Therefore, TEM imaging of the $A\beta_{1\text{-}40}$ aggregates in the presence or absence of hybrid-vesicles was performed (**Figure 6**). Incubation of monomeric $A\beta_{1\text{-}40}$ peptide during fibrillation with pure DOPC liposomes resulted in amyloid fibrils (Figure 6B). On the contrary, all hybrid DOPC-vesicles induced amorphous, less compacted fibrillar aggregates or no aggregates formation of monomeric peptide (Figure 6C-F and Supplementary Figure S6, Supporting Information).[59,60]

Structural transitions of the $A\beta_{1\text{-}40}$ peptide were further probed by far-UV circular dichroism (CD) spectroscopy. Fibrillation of the $A\beta_{1\text{-}40}$ peptide leads to a conformational shift from primary (negative minima at ≈200 nm) to secondary structures enriched with mainly β-sheet (negative signal ≈ 220 nm) containing fibrillar aggregates. Structural shifting to fibrillated structures, found in TEM images for $A\beta_{1\text{-}40}$ alone and in the presence of DOPC liposomes, was further confirmed by the indicated minima at ≈218 nm for β-sheet structures from CD-spectra. In contrast, the absence of this negative ≈218 nm signal indicates there was no or an only minor presence of fibrillar structures

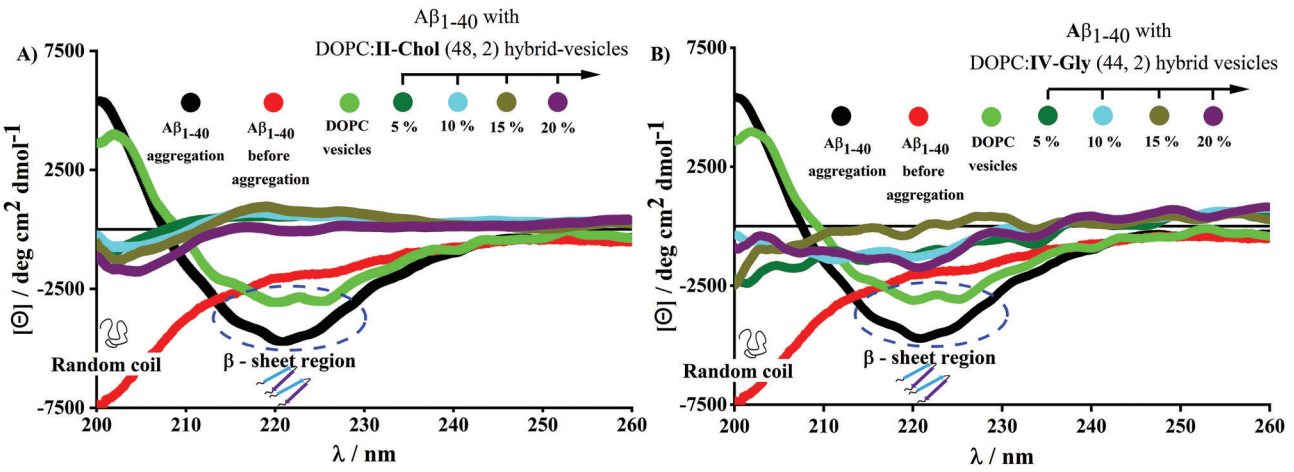

Figure 7. CD spectra of $A\beta_{1\text{-}40}$ either in the presence of polymers bearing hybrid-vesicles or pure DOPC vesicles, compared to the freshly prepared nonaggregated $A\beta_{1\text{-}40}$ peptide in 50 mM Na_2HPO_4 buffer (supplemented with 150 mM NaCl) pH 7.4. Inset of the plot shows molar percentage of polymers in hybrid liposomes. Mean residual ellipticities (MRE) of $A\beta_{1\text{-}40}$ peptide are recorded for hybrid liposomes containing A) **II-Chol** (48, 2) and B) **IV-Gly** (44, 2) polymers after ThT-dependent fibrillation assays. The transition from the random coil of native peptides to β-sheet enriched fibrils of mean residual ellipticity at 218 nm is displayed.

after interaction between hybrid-vesicles and the $A\beta_{1\text{-}40}$ peptide during fibrillation, as rather a small negative shifting of the CD-spectra ≈200 nm was observed. The morphological shift from fibrils to amorphous or no aggregates as observed in the TEM images, is thus further supported by CD-spectroscopy (see **Figure 7** and Figure S4, Supporting Information).

3. Conclusion

Herein we present a remarkable impact of cholesterol/diacylglycerol-polymer-hybrid-vesicles on the fibrillation of $A\beta_{1\text{-}40}$ peptides. We observe a clear retardation of fibrillation by the addition of hybrid-vesicles with both polymers in amounts of 5 – 20 mol% of added polymer. The suppression became more pronounced with the glycerol-anchored polymers bearing hybrid-vesicles compared to those bearing the cholesterol-anchor.

Apart from the strong retardation effect on fibrillation, a morphological shift (fibrils to amorphous) of the aggregates was observed. An explanation could be a nonproductive binding of the peptide to the hybrid-vesicles' water-accessible hydrophobic surface, responsible for exceeding the solubility limit of the peptide, ultimately transforming the peptide to amorphous aggregates via weak interactions like electrostatic and intermolecular interactions.[59,61] A further effect seems to be related to the hydrophobicity of the used polymers. Thus, polymers with a larger hydrophobic part show a less pronounced retardation, in comparison to those polymers displaying a shorter hydrophobic part, inline with a higher thermal transition.

Overall, this work demonstrates that the surface of the vesicles, decorated with hydrophilic polymers, can significantly alter amyloid $A\beta_{1\text{-}40}$ fibrillation. It is obvious that polymer embedded hybrid-vesicles can more efficiently bind to the primordial states of the amyloid protein, in turn inhibiting the formation of the cross β-sheets, as proven by the TEM and CD-spectroscopy. We now further exploit this attractive behavior by different hybrid-vesicles, bearing different polymers to investigate further more with other polymers bearing hybrid-vesicles and their influence on $A\beta_{1\text{-}40}$ fibrillation.

Supporting Information

Supporting Information is available from the Wiley Online Library or from the author.

Acknowledgements

The authors thank the Graduate School AGRIPOLY for the funding from the European Social Fund (ESF) and the state of Saxony-Anhalt; as well as the SFB TRR 102 / TP A012, project Nr 189853844, and funding from the Federal Ministry for Education and Resaearch (BMBF, 03Z22HI2).N.S has prepared the hybrid-vesicles, synthesized polymers, LCST measurement, and investigated the fibrillation kinetics assays. W.H.B designed research and analyzed data. The paper has written by N.S. and W.H.B. The authors would like to thank also Dr. Sven Rothemund for the synthesis of the native $A\beta_{1\text{-}40}$ peptide. C.H. has performed Confocal microscopy and G.H. performed TEM assays. The authors would like to thank Prof. Dr. Jochen Balbach for their valuable support.

Open access funding enabled and organized by Projekt DEAL.

Conflict of Interest

The authors declare no conflict of interest.

Data Availability Statement

The data that support the findings of this study are available in the supplementary material of this article.

Keywords

amphiphilic polymer, amyloid beta fibrillation, hybrid-vesicle

Received: November 29, 2022
Revised: February 18, 2023
Published online:

[1] J. Schnabel, *Nature* **2011**, *475*, S12.
[2] S. I. A. Cohen, S. Linse, L. M. Luheshi, E. Hellstrand, D. A. White, L. Rajah, D. E. Otzen, M. Vendruscolo, C. M. Dobson, T. P. J. Knowles, *Proc. Natl. Acad. Sci. U. S. A.* **2013**, *110*, 9758.
[3] M. Törnquist, T. C. T. Michaels, K. Sanagavarapu, X. Yang, G. Meisl, S. I. A. Cohen, T. P. J. Knowles, S. Linse, *Chem. Commun.* **2018**, *54*, 8667.
[4] J. Bieschke, M. Herbst, T. Wiglenda, R. P. Friedrich, A. Boeddrich, F. Schiele, D. Kleckers, J. M. Lopez Del Amo, B. A. Grüning, Q. Wang, M. R. Schmidt, R. Lurz, R. Anwyl, S. Schnoegl, M. Fändrich, R. F. Frank, B. Reif, S. Günther, D. M. Walsh, E. E. Wanker, *Nat. Chem. Biol.* **2011**, *8*, 93.
[5] K. Debnath, S. Shekhar, V. Kumar, N. R. Jana, N. R. Jana, *ACS Appl. Mater. Interfaces* **2016**, *8*, 20309.
[6] J. Mclaurin, R. Golomb, A. Jurewicz, J. P. Antel, P. E. Fraser, *J. Biol. Chem.* **2000**, *275*, 18495.
[7] F. L. Palhano, J. Lee, N. P. Grimster, J. W. Kelly, *J. Am. Chem. Soc.* **2013**, *135*, 7503.
[8] J. Habchi, P. Arosio, M. Perni, A. R. Costa, M. Yagi-Utsumi, P. Joshi, S. Chia, S. I. A. Cohen, M. B. D. Müller, S. Linse, E. A. A. Nollen, C. M. Dobson, T. P. J. Knowles, M. Vendruscolo, *Sci. Adv.* **2016**, *2*, e1501244.
[9] K. Dahse, M. Garvey, M. Kovermann, A. Vogel, J. Balbach, M. Fändrich, A. Fahr, *J. Mol. Biol.* **2010**, *403*, 643.
[10] P. M. H. Heegaard, U. Boas, D. E. Otzen, *Macromol. Biosci.* **2007**, *7*, 1047.
[11] B. Klajnert, J. Cladera, M. Bryszewska, *Biomacromolecules* **2006**, *7*, 2186.
[12] B. Klajnert, M. Cortijo-Arellano, J. Cladera, M. Bryszewska, *Biochem. Biophys. Res. Commun.* **2006**, *345*, 21.
[13] A. Assarsson, S. Linse, C. Cabaleiro-Lago, *Langmuir* **2014**, *30*, 8812.
[14] V. Castelletto, G. E. Newby, D. Hermida Merino, I. W. Hamley, D. Liu, L. Noirez, *Polym. Chem.* **2010**, *1*, 453.
[15] S. Dehn, V. Castelletto, I. W. Hamley, S. Perrier, *Biomacromolecules* **2012**, *13*, 2739.
[16] D. Ghosh, P. Dutta, C. Chakraborty, P. K. Singh, A. Anoop, N. N. Jha, R. S. Jacob, M. Mondal, S. Mankar, S. Das, S. Malik, S. K. Maji, *Langmuir* **2014**, *30*, 3775.
[17] S. Rocha, I. Cardoso, H. Börner, M. C. Pereira, M. J. Saraiva, M. Coelho, *Biochem. Biophys. Res. Commun.* **2009**, *380*, 397.
[18] Y. Song, P.-N. Cheng, L. Zhu, E. G. Moore, J. S. Moore, *J. Am. Chem. Soc.* **2014**, *136*, 5233.
[19] S. Funtan, Z. Evgrafova, J. Adler, D. Huster, W. Binder, *Polymers* **2016**, *8*, 178.
[20] S. A. Sorokina, Y. Y. Stroylova, Z. B. Shifrina, V. I. Muronetz, *Macromol. Biosci.* **2016**, *16*, 266.
[21] T. Takahashi, H. Mihara, *Acc. Chem. Res.* **2008**, *41*, 1309.
[22] A. Assarsson, E. Hellstrand, C. Cabaleiro-Lago, S. Linse, *ACS Chem. Neurosci.* **2014**, *5*, 266.
[23] M. Villmow, M. Baumann, M. Malesevic, R. Sachs, G. Hause, M. Fändrich, J. Balbach, C. Schiene-Fischer, *Biochem. J.* **2016**, *473*, 1355.
[24] B. Wang, E. H. Pilkington, Y. Sun, T. P. Davis, P. C. Ke, F. Ding, *Environ. Sci.: Nano* **2017**, *4*, 1772.
[25] D. Brambilla, R. Verpillot, B. Le Droumaguet, J. Nicolas, M. Taverna, J. Kóňa, B. Lettiero, S. H. Hashemi, L. De Kimpe, M. Canovi, M. Gobbi, V. Nicolas, W. Scheper, S. M. Moghimi, I. Tvaroška, P. Couvreur, K. Andrieux, *ACS Nano* **2012**, *6*, 5897.
[26] I. W. Hamley, *Chem. Rev.* **2012**, *112*, 5147.
[27] O. Press-Sandler, Y. Miller, *Protein Sci.* **2022**, *31*, e4283.
[28] D. J. Lindberg, E. Wesén, J. Björkeroth, S. Rocha, E. K. Esbjörner, *Biochim. Biophys. Acta Biomembr.* **2017**, *1859*, 1921.
[29] S. Andrade, J. A. Loureiro, M. C. Pereira, *ChemPhysChem* **2021**, *22*, 1547.
[30] C. Aisenbrey, T. Borowik, R. Byström, M. Bokvist, F. Lindström, H. Misiak, M.-A. Sani, G. Gröbner, *Eur. Biophys. J.* **2008**, *37*, 247.
[31] J.-M. Lin, T.-L. Lin, U.-S. Jeng, Z.-H. Huang, Y.-S. Huang, *Soft Matter* **2009**, *5*, 3913.
[32] H. Shao, S.-C. Jao, K. Ma, M. G. Zagorski, *J. Mol. Biol.* **1999**, *285*, 755.
[33] V. Rangachari, B. D. Moore, D. K. Reed, L. K. Sonoda, A. W. Bridges, E. Conboy, D. Hartigan, T. L. Rosenberry, *Biochemistry* **2007**, *46*, 12451.
[34] R. M. Murphy, *Biochim. Biophys. Acta. Biomembr.* **2007**, *1768*, 1923.
[35] N. Hu, L. Gao, Y. Jiang, S. Wei, S. Shang, C. Chen, L. Dang, J. Wang, K. Huo, M. Deng, J. Wang, Q. Qu, *Lipids Health Dis.* **2020**, *19*, 8.
[36] S. Grassi, P. Giussani, L. Mauri, S. Prioni, S. Sonnino, A. Prinetti, *J. Lipid Res.* **2020**, *61*, 636.
[37] C. L. Dias, S. Jalali, Y. Yang, L. Cruz, *J. Phys. Chem. B* **2020**, *124*, 3036.
[38] C. Di Scala, H. Chahinian, N. Yahi, N. Garmy, J. Fantini, *Biochemistry* **2014**, *53*, 4489.
[39] X. Yu, J. Zheng, *J. Mol. Biol.* **2012**, *421*, 561.
[40] J. Dai, M. Alwarawrah, J. Huang, *J. Phys. Chem. B* **2010**, *114*, 840.
[41] W. Gibson Wood, G. P. Eckert, U. Igbavboa, W. E. Müller, *Biochim. Biophys. Acta Biomembr.* **2003**, *1610*, 281.
[42] S.-R. Ji, Y. Wu, S.-F. Sui, *J. Biol. Chem.* **2002**, *277*, 6273.
[43] M. S. Terakawa, Y. Lin, M. Kinoshita, S. Kanemura, D. Itoh, T. Sugiki, M. Okumura, A. Ramamoorthy, Y.-H. Lee, *Biochim. Biophys. Acta Biomembr.* **2018**, *1860*, 1741.
[44] M. Sanguanini, K. N. Baumann, S. Preet, S. Chia, J. Habchi, T. P. J. Knowles, M. Vendruscolo, *ACS Chem. Neurosci.* **2020**, *11*, 1347.
[45] A. Vahdat Shariat Panahi, P. Hultman, K. Öllinger, G. T. Westermark, K. Lundmark, *Amyloid* **2019**, *26*, 34.
[46] Z. Niu, Z. Zhang, W. Zhao, J. Yang, *Biochim. Biophys. Acta Biomembr.* **2018**, *1860*, 1663.
[47] Z. Evgrafova, B. Voigt, A. H. Roos, G. Hause, D. Hinderberger, J. Balbach, W. H. Binder, *Phys. Chem. Chem. Phys.* **2019**, *21*, 20999.
[48] Z. Evgrafova, B. Voigt, M. Baumann, M. Stephani, W. H. Binder, J. Balbach, *Chemphyschem* **2019**, *20*, 236.
[49] Z. Evgrafova, S. Rothemund, B. Voigt, G. Hause, J. Balbach, W. H. Binder, *Macromol. Rapid Commun.* **2019**, *41*, 1900378.
[50] N. Sen, G. Hause, W. H. Binder, *Macromol. Rapid Commun.* **2021**, *42*, 2100120.
[51] M. S. Terakawa, H. Yagi, M. Adachi, Y.-H. Lee, Y. Goto, *J. Biol. Chem.* **2015**, *290*, 815.
[52] J. Habchi, S. Chia, C. Galvagnion, T. C. T. Michaels, M. M. J. Bellaiche, F. S. Ruggeri, M. Sanguanini, I. Idini, J. R. Kumita, E. Sparr, S. Linse, C. M. Dobson, T. P. J. Knowles, M. Vendruscolo, *Nat. Chem.* **2018**, *10*, 673.
[53] E. London, G. W. Feigenson, *J. Lipid Res.* **1979**, *20*, 408.
[54] I. M. Armitage, D. L. Shapiro, H. Furthmayr, V. T. Marchesi, *Biochemistry* **1977**, *16*, 1317.
[55] P. L. Yeagle, *eMagRes* **2019**, *1115*, 99.
[56] M. Schulz, S. Werner, K. Bacia, W. H. Binder, *Angew. Chem. Int. Ed. Engl.* **2013**, *52*, 1829.
[57] M. Schulz, D. Glatte, A. Meister, P. Scholtysek, A. Kerth, A. Blume, K. Bacia, W. H. Binder, *Soft Matter* **2011**, *7*, 8100.
[58] M. Grimmer, K. Bacia, *Sci. Rep.* **2020**, *10*, 3100.
[59] Y. Yoshimura, Y. Lin, H. Yagi, Y.-H. Lee, H. Kitayama, K. Sakurai, M. So, H. Ogi, H. Naiki, Y. Goto, *Proc. Natl. Acad. Sci. U. S. A.* **2012**, *109*, 14446.
[60] J. Wu, N. Österlund, H. Wang, R. Sternke-Hoffmann, H. Pupart, L. L. Ilag, A. Gräslund, J. Luo, *Cell Rep. Phys. Sci.* **2022**, *3*, 101018.
[61] D. Jiang, I. Rauda, S. Han, S. Chen, F. Zhou, *Langmuir* **2012**, *28*, 12711.